Antiviral Research 172 (2019) 104644

Contents lists available at ScienceDirect

Antiviral Research

journal homepage: www.elsevier.com/locate/antiviral

A synthetic derivative of houttuynoid B prevents cell entry of Zika virus

Michael Basic[a,1], Fabian Elgner[a,1], Daniela Bender[a], Catarina Sabino[a], Marie-Luise Herrlein[a], Hanna Roth[a], Mirco Glitscher[a], Alicia Fath[a], Thomas Kerl[b], Hans-Günther Schmalz[b], Eberhard Hildt[a,c,*]

[a] Paul-Ehrlich-Institut, Dept. of Virology, 63225, Langen, Germany
[b] Department of Chemistry University of Cologne, 50939, Koeln, Germany
[c] German Center for Infection Research (DZIF), 38124, Braunschweig, Germany

ARTICLE INFO

Keywords:
Houttuynoid
Zika virus
Flavivirus
Antiviral activity
Natural compounds
Flavonoids

ABSTRACT

Zika virus (ZIKV) is a re-emerging virus belonging to the family of *Flaviviridae*, which contains several human pathogens. A great deal of attention came through the association of ZIKV infection with an increasing number of microcephaly cases in newborns during the 2016 outbreak in Brazil. Currently, no anti-viral drug or vaccine is available.

Houttuynoids are a group of structurally related flavonoid glycosides that can be isolated from *Houttuynia cordata* belonging to the family of *Sauraceae*. Moreover, *H. cordata* was described to have an antiviral effect on herpes simplex virus type 1 (HSV-1), human immunodeficiency virus type 1 (HIV-1) and influenza A virus (Hayashi et al., 1995). In light of this, this study aimed to investigate a potential antiviral effect of the synthetic houttuynoids TK1023 and TK1024 (i.e. houttuynoid B) on two ZIKV isolates (Uganda and French Polynesia).

A significant decrease in the amount of intra- and extracellular viral genomes as well as infectious viral particles was observed after treatment with the tetra-O-acetylated houttuynoid TK1023 independent from the analyzed virus isolate. In contrast, TK1024 (houttuynoid B) had no effect on ZIKV. Treatment with TK1023 significantly decreases the number of infected cells 24 h and 48 h after infection, as compared to the control. Analysis of the mode of action revealed that TK1023 neither affects the viral genome replication nor the production of viral proteins nor morphogenesis or release. Binding and entry assays showed that TK1023 interferes with the entry of the virus in the cell. Thereby, the spread of ZIKV infection is impaired as the infection of the individual cell is inhibited.

These data indicate that for both analyzed virus isolates the spread of ZIKV infection can be impaired by the synthetic houttuynoid TK1023 due to an inhibition of the viral entry.

1. Introduction

Zika virus (ZIKV) is an arbovirus belonging to the genus Flavivirus within the family of *Flaviviridae* and was first isolated in 1947 from a rhesus monkey in the Zika forest in Uganda (Dick et al., 1952). The first infection of humans was described in 1954 in Nigeria (MacNamara, 1954), following a period of over 50 years where only a few cases of human infections were reported (Faye et al., 2014). The first outbreak took place in 2007 on the island of Yap in Micronesia followed by an epidemic in French Polynesia in 2013/2014 (Duffy et al., 2009; Cao-Lormeau et al., 2014). International attention focused on ZIKV during the large outbreak in Brazil and South America when ZIKV infection during pregnancy was linked to congenital microcephaly. Moreover, an association of ZIKV infection with Guillain-Barré syndrome (GBS) was observed (Zanluca et al., 2015; Cao-Lormeau et al., 2016; Schuler-Faccini et al., 2016). In light of this, the World Health Organization (WHO) declared a Public Health Emergency of International Concern (PHEIC) in February 2016 (WHO, 2016).

Transmission of ZIKV to humans primarily occurs by *Aedes* mosquitos (*Aedes aegypti* and *Aedes albopictus*). Alternatively, transmission can occur via sexual contact, blood transfusions or from the mother to the child (Sharma and Lal, 2017).

* Corresponding author. Paul-Ehrlich-Institut, Dept. of Virology, 63225, Langen, Germany.
E-mail addresses: Michael.basic@kgu.de (M. Basic), Fabian.Elgner@pei.de (F. Elgner), Daniela.Bender@pei.de (D. Bender), Catarina.Sabino@pei.de (C. Sabino), Marie-Luise.Herrlein@pei.de (M.-L. Herrlein), Hanna.Roth@pei.de (H. Roth), Mirco.Glitscher@pei.de (M. Glitscher), Alicia.Fath@pei.de (A. Fath), Kerl@uni-koeln.de (T. Kerl), Schmalz@uni-koeln.de (H.-G. Schmalz), Eberhard.Hildt@pei.de (E. Hildt).
[1] Equal contribution.

https://doi.org/10.1016/j.antiviral.2019.104644
Received 24 June 2019; Received in revised form 30 October 2019; Accepted 2 November 2019
Available online 04 November 2019
0166-3542/

ZIKV possesses a (+)-stranded single stranded (ss) RNA genome with a size of approximately 11 kb. The 5' – and 3' –ends harbor untranslated regions which are highly structured and essential for viral replication and translation. A single open reading frame encompasses the whole genome and yields a long polyprotein with 3419 amino acids (aa) or 3410 aa for the Uganda or the French Polynesia isolate, respectively. Subsequent processing of the polyprotein is mediated by viral and host proteases resulting in the formation of three structural proteins, the core protein (C), the pre-membrane protein (prM), which is further processed by furin proteases to the M protein, and the envelope protein (E), as well as seven non-structural proteins (NS1, NS2A, NS2B, NS3, NS4A, NS4B, NS5). The viral RNA-dependent RNA polymerase (NS5) contains a methyltransferase domain, crucial for the 5′-capping of the viral RNA (Kuno and Chang, 2007; Baronti et al., 2014; Coutard et al., 2017).

Houttuynoids are a group of structurally related flavonoid glycosides with a unique benzofuran moitey originally isolated in 2012 from *Houttuynia cordata*, a plant belonging to the family of *Sauraceae* (Chen et al., 2012). *H. cordata* is used as a medicinal plant in traditional Chinese medicine and known as "Yu-Xing-Cao" to treat fever, reduce swelling and to drain pus. Moreover, a steam distillate from *H. cordata* was described to have an antiviral effect on herpes simplex virus type 1 (HSV-1), human immunodeficiency virus type 1 (HIV-1) and influenza A virus (Hayashi et al., 1995; Li et al., 2005). Further investigation revealed that the antiviral activity is based on the houttuynoids as active metabolites. A detailed analysis demonstrated an antiviral effect of isolated houttuynoids on HSV. In light of the antiviral activity of the houttuynoids and their limited availability, strategies for the chemical synthesis of houttuynoid B and A (Kerl et al., 2016; Jian et al., 2018) were pursued to allow the production of these compounds and synthetic derivatives. This enabled a more thorough study of the antiviral activity of tetra-acetyl-houttuynoid B (TK1023) and the parent substance houttuynoid B (TK1024) (Kerl et al., 2016) (Fig. 1).

So far there is neither a preventive vaccine nor a specific robust therapy to control ZIKV infection available. This study aims to investigate the antiviral potential of two synthetic houttuynoids on the ZIKV life cycle and to delineate the mechanism of the antiviral effect on ZIKV.

2. Materials and methods

2.1. Cell culture

African green monkey kidney cells (Vero, Vero E6), human epithelial lung carcinoma cells (A549) and the human hepatocellular cell line Huh7.5 were grown in Dulbecco's Modified Eagle's medium (DMEM) complete which represents DMEM High Glucose (BioWest, Nuaillé, France) supplemented with 10% Fetal Bovine Serum Superior (Biochrom GmbH, Berlin, Germany), 2 mM L-Glutamine (Biochrom GmbH, Berlin, Germany), 100 U/mL penicillin and 100 µg/mL streptomycin (Paul-Ehrlich-Institut facilities, Langen, Germany) in a humidified incubator at 37 °C with 5% CO_2. Passaging of the cells was performed by trypsinization three times a week.

2.2. Infections

Two ZIKV isolates were used in this study: the isolate French Polynesia PF13/251013–18 ("Polynesia") and the Uganda 976 strain ("Uganda") of ZIKV, which were kindly provided by Dr. Didier Musso from the Institute Louis Malardé, Tahiti, and the European Virus Archive, respectively. A549 cells were infected with a multiplicity of infection (MOI) of 0.1 or 1 for 16 h. Then, the inoculum was removed and the cells were washed once with PBS. Cell culture supernatants were collected at the indicated time points and subjected to further analyses.

The West Nile Virus (WNV) isolate NY-99 was used to infect Vero E6 cells at an MOI of 1 for 16 h.

In addition, the A549 subclone A549/D3 was infected with HEV strain 47832c at an MOI of 10 for 16 h. Both the cells and the virus were described before (Glitscher et al., 2018). Cell culture-derived HEV exists as "quasi-enveloped" virus. Therefore the virions were treated with 250 mM taurocholic acid and purified by density gradient centrifugation. The density of the isolated virus used for subsequent infection corresponds to the naked, non-enveloped virus.

Moreover, a luciferase reporter virus was used. Here, the coding sequence for the *Renilla* luciferase reporter is inserted in the ZIKV genome. After translation of the polyprotein, the luciferase is released from the polyprotein during the processing. The RNA encoding the reporter virus was generated by in vitro transcription of the plasmid pFLZIKV-RLuc that was kindly provided by Dr. Robert Tesh's World Reference Center of Emerging Viruses and Arboviruses (WRCEVA)

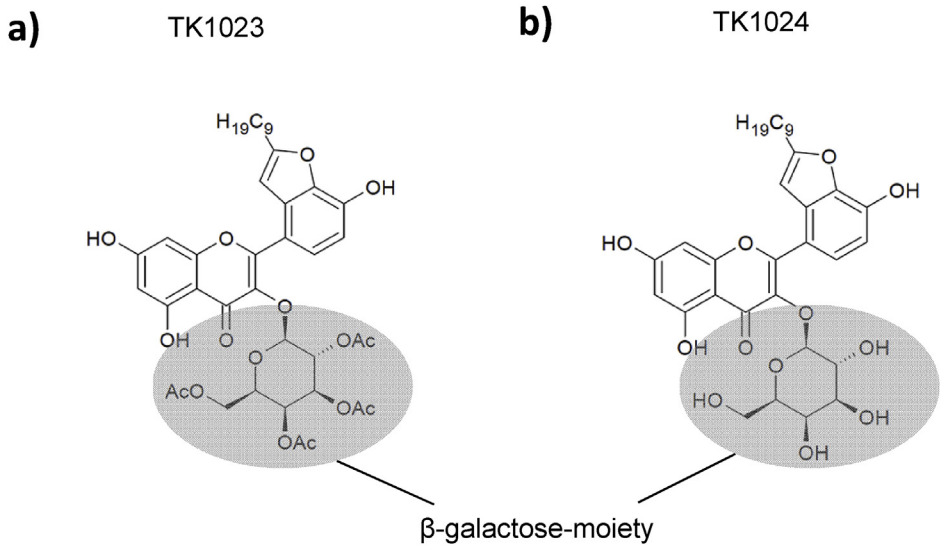

Fig. 1. Structure of synthetic houttuynoids TK1023 and TK1024 (identical to houttuynoid B)
Structures of TK1023 (a) and TK1024 (b).

through the University of Texas Medical Branch, Galveston, Texas 77555, USA and subjected to subsequent capping. A detailed characterization of this construct is given in (Shan et al., 2016). Transfection of A549 cells was performed by electroporation of 10 µg RNA by using a Gene Pulser MXcell™ (BioRad, USA) delivering one single pulse at 300 V and 950 µF. After two passages, the luciferase signal was stable and almost all cells were infected as evidenced by immunofluorescence microscopy. Luciferase activity was determined by using the Gaussia GLOW-Juice Luciferase assay kit (PJK GmbH, Kleinblittersdorf, Germany).

The HCV RNA of the chimeric isolate Jc1 was generated by T7 in vitro transcription and electroporation into Huh7.5 cells was performed as described (Elgner et al., 2016).

2.3. Treatments

In general, infected cells were treated for 2 h prior to infection with the two synthetic houttuynoids TK1023 and TK1024. TK1023 might be considered a prodrug variant of TK1024 as it contains a per-acetylated sugar (β-galactose) moiety. The structures of the two compounds are shown in Fig. 1. Synthesis of these compounds was described recently (Kerl et al., 2016). If not indicated, the houttuynoids were permanent present and were renewed at 16, 40, and 64 h post-infection (hpi) to ensure constant levels of the substance in cells and media after washing steps. Treatment with the respective amount of the vehicle control, DMSO (Genaxxon Bioscience GmbH, Ulm, Germany) served as control.

In case of virus pre-incubation, ZIKV Uganda virions were incubated with 5 µM TK1023, 50 nM bafilomycin A (BFLA) or 0.05% DMSO for 2 h at 37 °C. Afterwards, the inoculum was diluted 40-fold in DMEM complete resulting in an MOI of 1 and dilution of the respective substance below working concentration.

The time-of-addition assay was performed as described (Gaudry et al., 2018). In brief, A549 cells were infected with ZIKV at an MOI of 0.1 for 16 h and viral genomes were quantified 24 hpi. TK1023 was present in a concentration of 5 µM throughout the whole experiment starting with 2 h pre-incubation (TO), only during the 2 h of infection (CoT), only during the 2 h before the infection (Pre) or added 2 h after the infection (post). In a different approach, the cells were infected with ZIKV “Uganda” at a MOI of 1 and the substances BFLA (50 nM), silvestrol (5 nM), TK1023 (5 µM) or DMSO (0.05%) were added 0, 1, 2, 4, 6 or 23 hpi. The amount of intracellular viral genomes was quantified by qPCR 24 hpi. The recovery of the ZIKV-specific signal represents the step of the viral life cycle, at which the respective inhibitory substance acts on.

2.4. Binding and entry assays

Binding: A549 cells were precooled for 30 min at 4 °C before infection for 1 h with the ZIKV strain “Uganda” at an MOI of 1 to allow binding of virions while inhibiting the entry step. Simultaneously, the cells were treated with 5 µM of TK1023. Subsequently, the cells were harvested in Trifast for quantification of the intracellular ZIKV genomes by qPCR.

Entry: A549 cells were infected with the ZIKV strain “Uganda” at an MOI of 1 for 4 h at 37 °C in presence of 5 µM of TK1023. Bound but not entered virions were removed by trypsin treatment for 30 s at room temperature. Subsequently, the RNA was extracted, reverse transcribed into cDNA and the intracellular ZIKV genomes of entered virions quantified by qPCR as described below.

2.5. Virus titration

Quantification of infectious virus was performed by plaque assay. Vero cells were infected with 100 µL of serial dilutions of either cleared cell lysate or supernatant. To quantify intracellular viral particles, the cells were lysed by three cycles of freeze-thaw at −80 °C and at 37 °C. The lysate was cleared by a 10 min centrifugation step at 5000 g at 4 °C. 2 hpi, the inoculum was removed and 0.4% SeaPlaque® agarose (Lonza, Basel, Switzerland) in DMEM complete was carefully layered over the cells. The agarose overlay was kept at room temperature for 15 min to allow solidification. The plaques were visualized 5 days after infection as described (Elgner et al., 2018). The virus titers were expressed in plaque-forming units per mL (pfu/mL). The half maximal inhibitory concentration (IC_{50}) values were calculated by non-linear regression fitting of the normalized plaque-forming units and the log-transformed concentrations using the software GraphPad Prism 7 (GraphPad Software, La Jolla, USA).

2.6. Quantification of viral genomes, RNA isolation and cDNA synthesis

Total intracellular RNA was isolated from infected cells using peqGOLD TriFast (PEQLAB Biotechnologie GmbH, Erlangen, Germany) according to the manufacturer's instructions. DNase treatment, reverse transcription and qPCR were performed as described (Elgner et al., 2018). In brief, cDNA was quantified in a LightCycler480 (Roche, Basel, Switzerland) using SYBR-green (Thermo Fisher Scientific, Waltham, USA) and specific primers for ZIKV, HCV, HEV and RPL27. The sequences of the used primers were as follows: RPL27_fwd: aaagctgtcatcgtgaagaac; RPL27_rev: gctgtcactttgcgggggtag; ZIKV_fwd: agatcccggctgaaacactg; ZIKV_rev: ttgcaaggtccatctgtccc; HCV_fwd: atgaccacaaggcctttcg; HCV_rev: cgggagagccatagtgg; HEV_fwd: ggtggtttctggggtgac; HEV_rev: aggggttggttggatgaa. The amount of viral genomes was determined by the ΔΔcp-method with normalization on the housekeeping gene RPL27The amount of viral genomes was determined by the ΔΔcp-method with normalization on the housekeeping gene RPL27. For isolation of extracellular RNA, the QIAamp Viral RNA Mini Kit (Qiagen, Hilden, Germany) was used according to the manufacturer's protocol. Quantification of the extracellular viral genomes was performed by qPCR using the Zika Virus detection kit (TIB Molbiol, Berlin, Germany) together with the LightCycler Multiplex RNA Virus Mastermix (Roche, Basel, Switzerland) in a LightCycler480 (Roche, Basel, Switzerland) as described (Elgner et al., 2018).

2.7. Cell viability

For determination of cell viability after treatment with the houttuynoids TK1023 and TK1024, the PrestoBlue® Cell Viability Reagent (Thermo Fischer Scientific, Waltham, USA) was used as described by the manufacturer. A549 cells were seeded in flat-bottom polystyrene 96-well plates (Greiner, Frickenhausen, Germany), at a density of 1×10^4 cells per well, and treated with different concentrations of the compounds for the indicated times. Treatment with 1% Triton X-100 (Sigma-Aldrich, St.Louis, USA) served as a positive control. The microplate reader Infinite M1000 (Tecan, Basel, Switzerland) was used for measurement of the fluorescence of the reagent after 1 h of incubation at 37 °C. The mean cytotoxic concentration (CC_{50}) values were calculated by non-linear regression fitting of the normalized viability data and the log-transformed concentrations using the software GraphPad Prism 7 (GraphPad Software, La Jolla, USA).

2.8. Western blot

SDS-PAGE and Western blot analyses were performed as described (Elgner et al., 2018). NS1 was detected using anti-ZIKV NS1 (1:1000; BioFront Technologies, Tallahassee, USA). Detection of β-Actin (1:10000; Sigma-Aldrich, St.Louis, USA) served as a loading control. As secondary antibodies, either a horseradish peroxidase (HRP)-coupled antibody (GE Healthcare, Little Chalfont, United Kingdom) or a fluorophore-coupled antibody (LI-COR Biosciences, Lincoln, USA) was used. For detection, Luminata Forte Western HRP Substrate (Merck Millipore, Darmstadt, Germany) and scientific imaging films (GE Healthcare, Little Chalfont, United Kingdom) were used or the LI-COR Odyssey

infrared imaging system (LI-COR Biosciences, Lincoln, USA). The NS1-specific signal was quantified with the LI-COR software ImageStudio (LI-COR Biosciences, Lincoln, USA) and normalized to the intensities of the respective beta-actin band.

2.9. Confocal laser scanning microscopy

Cells were grown on coverslips and fixed with 4% formaldehyde in PBS for 20 min at room temperature. Permeabilization and blocking were performed as described (Elgner et al., 2018). Cells were incubated with anti-Flavivirus Group antigen antibody, clone D1-4G2-4-15 (1:300; Merck Millipore, Darmstadt, Germany) or anti-ZIKV NS1 (1:1000; BioFront Technologies, Tallahassee, USA). Afterwards, cells were incubated with anti-mouse IgG-Alexa 488 (1:1000; Thermo Fisher Scientific, Waltham, USA). Nuclei were visualized with 4′,6-diamidino-2-phenylindole (DAPI) (Carl Roth, Karlsruhe, Germany). The coverslips were mounted on microscope slides with Mowiol and analyzed using the confocal laser scanning microscope LSM 510 Meta and ZEN 2009 software (Carl Zeiss, Oberkochen, Germany).

2.10. Statistical analysis

Results are described as mean ± standard error of the mean (SEM) from at least 3 independent experiments. The significance of the results was analyzed by Student's t-test using GraphPad Prism 7 (GraphPad Software, La Jolla, USA). Ns = not significant; $p > 0.05$; *$p < 0.05$; ***$p < 0.001$; ****$p < 0.0001$.

3. Results

3.1. The houttuynoids TK1023 and TK1024 exert no cytotoxic effect on A549 cells

To test the effect of the houttuynoids TK1023 and TK1024 on the cell viability, A549 cells were treated with 10 nM, 100 nM, 1 μM and 5 μM of the respective substance for 72 h. Treatment with 0.1% DMSO served as vehicle control, 35 μM cycloheximide (CHX) and 1% Triton X-100 served as additional controls. The medium with the inhibitors/substances was changed every 24 h. The viability measured by Prestoblue assay and the relative viability was determined by comparison to untreated cells (w/o) (Fig. 2a).

Cell viability was not reduced even at highest working concentrations. Additionally, the CC_{50} was determined for both substances (Fig. 2b). The CC_{50} values for TK1023 and TK1024 were established at 6.3 μM and 42.5 μM respectively. These concentrations are above the highest concentration tested by Prestoblue assay. The concentration of 5 μM was chosen for further experiments with both substances.

3.2. Decreased amount of intra- and extracellular viral RNA in TK1023 treated cells

To investigate the impact of TK1023 and TK1024 on ZIKV life cycle, A549 cells were infected with an MOI of 0.1 either with the French Polynesia (P) or the Uganda (U) ZIKV isolate and treated for 24, 48 or 72 h with 5 μM of the substances. DMSO-treated cells served as control.

The number of intra- and extracellular viral genomes was determined by qPCR. TK1024, the deacetylated compound, failed to exert any significant inhibitory effect on the intra- and extracellular amount of viral genomes for both virus strains at all time points investigated (Fig. 2c and d).

In contrast, a strong decrease in the number of intracellular and extracellular genomes was observed for both isolates when treated with the acetylated compound (TK1023) at 24 h. After 48 h, the effect was less pronounced and disappeared after 72 h (Fig. 2c and d).

For further characterization of this effect, the amount of NS1 was determined by Western blot analysis and subsequent quantification (Fig. 2e). Cells treated with either TK1023 or TK1024 were harvested after 24, 48 and 72 h of infection and subsequently lysed. DMSO treated cells served as control. Again, no inhibitory effect on the NS1 formation was detected for cells treated with TK1024. However, cells treated with TK1023 displayed a reduction in the amount of NS1 after 24 h. After 48 h, the effect of TK1023 on the amount of NS1 had already diminished when compared to 24 h and completely receded after 72 h. These effects were observed for both virus isolates (Fig. 2e).

Taken together, these data indicate that TK1023 initially exerts a significant effect on the number of intracellular and extracellular viral genomes, as well as on the amount of the viral nonstructural protein NS1. However, this effect vanishes over a timeframe of 72 h.

3.3. TK1023 decreases number of intra- and extracellular infectious viral particles

As described recently, the number of viral genomes does not necessarily reflect the number of infectious viral particles (Himmelsbach and Hildt, 2018). To investigate the effect of TK1024 and TK1023 on the number of intracellular and extracellular viral particles, plaque assays for absolute quantification of the infectious viral particles at 24 h (Fig. 3a), 48 h (Fig. 3b) and 72 h (Fig. 3c) after infection/treatment were performed. No significant inhibitory effect on the number of intracellular or extracellular viral particles could be observed for TK1024 at the investigated time points and for both isolates. TK1023 led to a strong decrease in the number of intracellular and extracellular infectious viral particles for both isolates, which was more pronounced for the Uganda strain. 48 h after infection there was still a discernible reduction in the number of intra- and extracellular infectious viral particles. However, the effect rapidly diminished and almost disappeared at 72 h (Fig. 3c). These data indicate that TK1023 leads to a strong decrease in the number of intra- and extracellular viral particles in the early phase of the infection.

3.4. The half-maximal effective concentration of TK1023 is lower than 2 μM

To further characterize the effect of TK1023 and TK1024 the half-maximal effective concentration (EC_{50}) for both substances was determined. To establish the EC_{50}, A549 cells were treated with different concentrations of TK1023 or TK1024 and infected with an MOI of 1, either with the Polynesia or the Uganda strain for 24 h. The cells were subsequently lysed and used to ascertain the number of infectious viral particles via plaque assay (Fig. 4). For TK1023, the detected EC_{50} values for the Polynesia and the Uganda strain were below the concentration used for the experiments, namely at 1.675 μM and 1.552 μM respectively. TK1024 displayed no inhibition in the tested range of concentrations for the Polynesia strain and a significantly higher EC_{50} value than 5 μM for the U strain at 25.8 μM. Taken together, this shows that the chosen working concentration of TK1023 is well above the EC_{50} value for both strains.

3.5. TK1023 impairs the infection by ZIKV

As the experiments were performed at a low MOI (0.1), we hypothesized that the observed effect reflects an impaired spread of the infection. To study this hypothesis, A549 cells were treated with the inhibitors TK1023 or TK1024 and infected with either the Uganda strain (Fig. 5a–c) or the French Polynesia strain (Fig. 5d–f) with an MOI of 0.1. The cells were fixed 24 h (Fig. 5a, d), 48 h (Fig. 5b, e) and 72 h (Fig. 5c, e) after infection and the number of positive cells was determined by immunofluorescence microscopy using an NS1-specific antiserum. The analysis revealed an overall lower number of infected cells for both strains (Uganda Fig. 5a and Polynesia Fig. 5d) if the cells were treated with TK1023 for 24 h. At the chosen concentration of 5 μM, there is no complete block of infection. In light of this, secondary

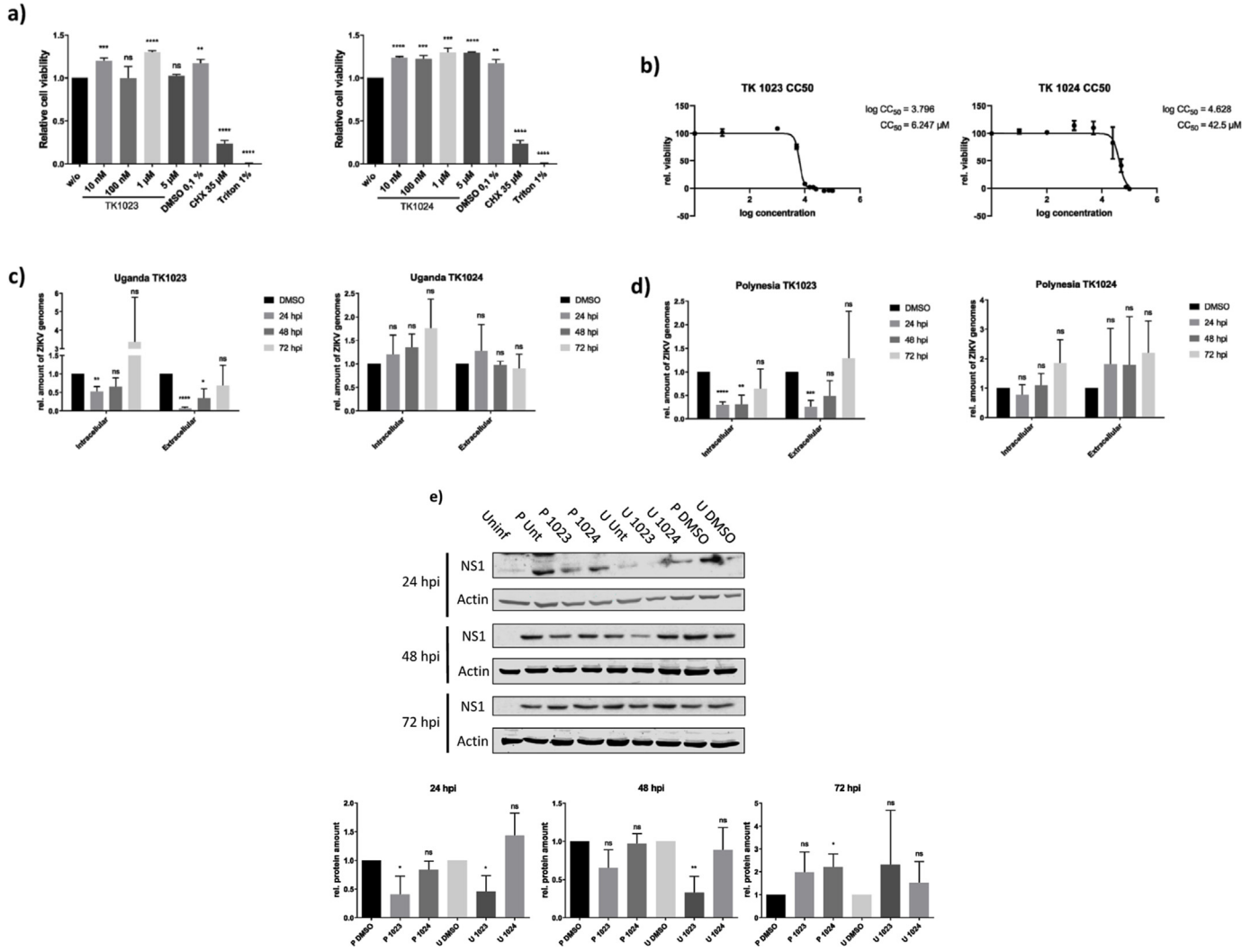

Fig. 2. Decreased amount of intra- and extracellular viral RNA in TK1023 treated cells

(a) A549 cells were treated with 10 nM, 100 nM, 1 µM and 5 µM of TK1023 or TK1024 for 24, 48 and 72 h. The relative cell viability was determined using the PrestoBlue assay. All relative values were normalized to untreated (w/o) cells. Cycloheximide (CHX) and 1% of Triton X-100 were included as positive controls.
(b) Calculated CC50 values of TK1023 and TK1024 based on the viability data shown in (a)(c/d) A549 cells were infected with the ZIKV strains "Uganda" (c) or "Polynesia" (d) at an MOI of 0.1 and treated with 5 µM of TK1023, TK1024 or DMSO (0.1%). All relative values shown were normalized to the respective DMSO control for each time point. Intracellular ZIKV genomes were quantified relative to a house-keeping gene by qPCR 24, 48 and 72 hpi.
(e) The amount of viral NS1 protein was assessed by Western blot analysis 24, 48 and 72 hp
i. One representative blot is shown. The quantification is based on three independent experiments. P = ZIKV Polynesia; U = ZIKV Uganda
Results are described as mean ± standard error of the mean (SEM) from 3 independent experiments. The significance of the results was analyzed by Student's t-test. ns = not significant; $p > 0.05$; *$p < 0.05$; ***$p < 0.001$; ****$p < 0.0001$.

spread by cell to cell transmission can occur based on de novo synthesized virions emerging from even few primary infected cells. Therefore, after 48 h a spread of the infection can be observed for the TK1023-treated cells, showing an increase in the number of NS1 positive cells (Fig. 5b, e). The strongest production of viral NS proteins occurs during early infection of a cell, after which it decreases. Considering this, there is a stronger intensity of the NS1-specific signal for the secondary-infected cells that were infected more recently. Finally, after 72 h most cells were positive for NS1 regardless of the treatment (Fig. 5c, f). Once more, there is a stronger NS1-specific signal for the secondary- or tertiary-infected cells that were treated while the NS1-specific signal in the control cells is much lower due to the fact that infection was not hindered and infection of most cells was achieved much earlier. This reflects the fact that over the infection time of 72 h the NS1-specific signal decreases. In accordance with the previous data, treatment with TK1024 did not affect the number of ZIKV-positive cells when compared to the control.

Taken together, these data indicate that the houttuynoid TK1023 affects the establishment of ZIKV infection, but has no effect on an already infected cell.

3.6. Replication of ZIKV is not affected by the houttuynoid TK1023

The data described above demonstrate that treatment with TK1023 leads to a smaller number of ZIKV-positive cells in the early phase of the infection. However, positive cells displayed similar amounts of NS1that was studied as replication marker, suggesting that the antiviral effect of TK1023 is not due to direct interference with the viral replication. To control this experimentally, cells were transfected with the ZIKV luciferase reporter genome that allows a direct analysis of viral replication, which is reflected by the luciferase activity. After transfection of the cells with the reporter virus, cells were passaged twice to ensure that all cells contain the reporter virus as indicated by a stable luciferase activity between passages. Treatment of these cells for up to 24 h with

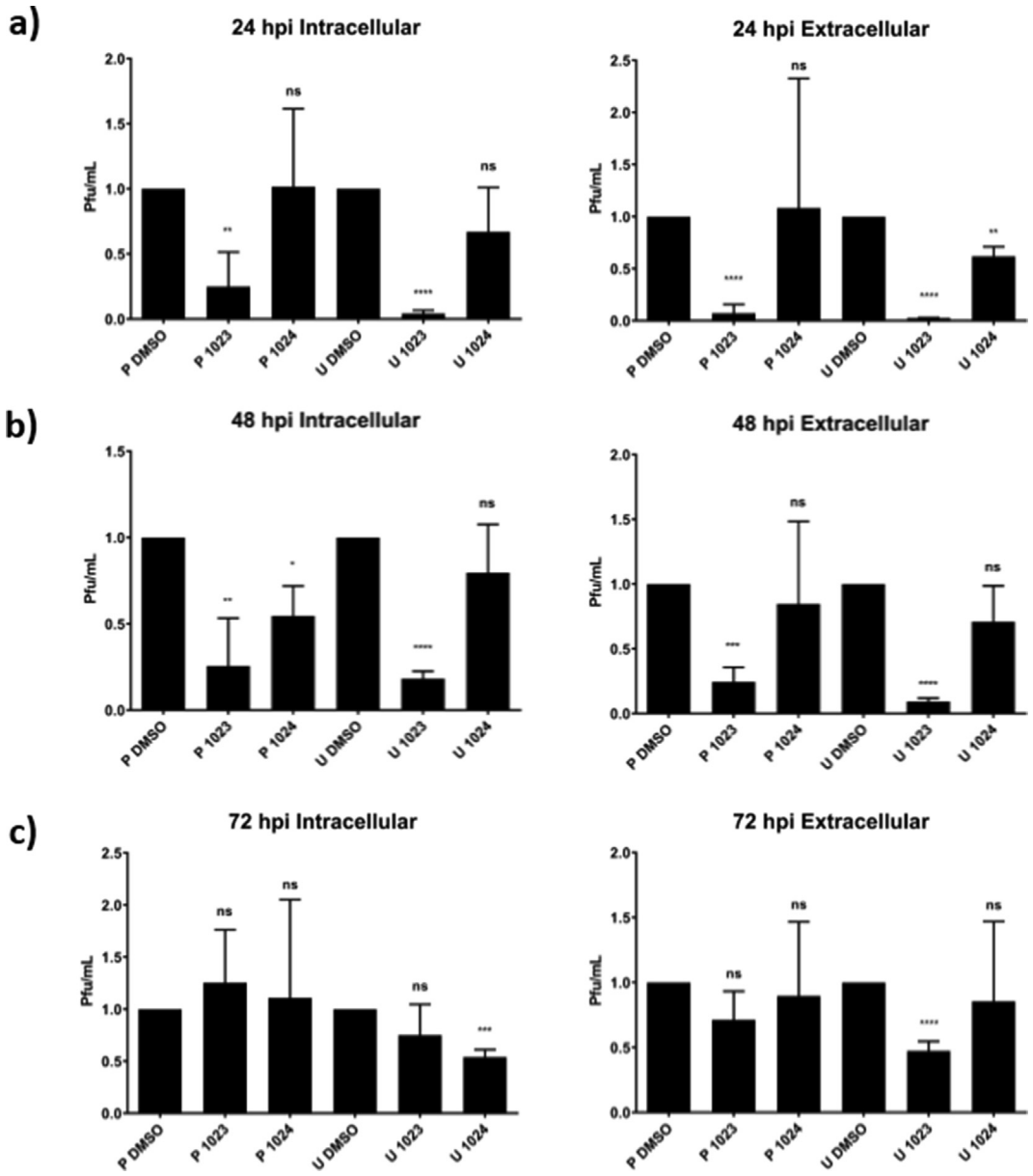

Fig. 3. TK1023 decreases the amount of released infectious viral particles

A549 cells were infected with the ZIKV strains "Uganda" or "Polynesia" at an MOI of 0.1 and treated with 5 μM of TK1023, TK1024 or DMSO (0.1%). The number of infectious intra– and extracellular virions at 24 h (a), 48 h (b) and 72 h (c) were quantified by plaque assay using Vero cells. Relative numbers are shown that are referred to the DMSO treated controls. The data are based on three independent experiments. P = ZIKV Polynesia; U = ZIKV Uganda

Results are described as mean ± standard error of the mean (SEM) from 3 to 5 independent experiments. The significance of the results was analyzed by Student's t-test. ns = not significant; $p > 0.05$; *$p < 0.05$; ***$p < 0.001$; ****$p < 0.0001$.

TK1023 and subsequent analysis of the luciferase activity in treated and untreated cells revealed that TK1023 had no significant effect on the luciferase activity (Fig. 6a).

These data indicate that TK1023 does not affect ZIKV replication.

3.7. The houttuynoid TK1023 blocks ZIKV entry in the target cell

The experiments described above demonstrate that neither the genome replication nor the release of infectious viral particles are affected by the treatment with TK1023. The delayed establishment of the viral infection in TK1023-treated cells could be due to an impaired binding or entry of ZIKV. In light of this, binding and entry assays of ZIKV in TK1023-treated cells were performed. DMSO-treated cells served as control. The binding assays revealed that the attachment of ZIKV to A549 cells is not significantly affected by the presence of TK1023. In contrast to this, the entry assay showed that TK1023 impairs the entry of ZIKV (Fig. 6b). Thus, we conclude that the inhibitory effect of TK1023 on the establishment of ZIKV infection is due to impaired entry. This prevents, on the one hand, the efficient establishment of the initial infection but does not completely block it and on the other hand, the spread of the virus due to secondary infection by de novo synthesized virions.

As the inhibitory effect of TK1023 vanished over time, we investigated at which time point after infection the compound loses its antiviral activity by a time-of-addition-assay. For this purpose, A549 cells were infected with an MOI of 1 with the Uganda strain and treated with either BFLA, silvestrol, DMSO or TK1023 at the indicated time points up to 24 h (Fig. 6c). The assay revealed that BFLA inhibited early ZIKV infection corresponding to its already established effect as an entry inhibitor (Sabino et al., 2019). Addition of silvestrol, a known

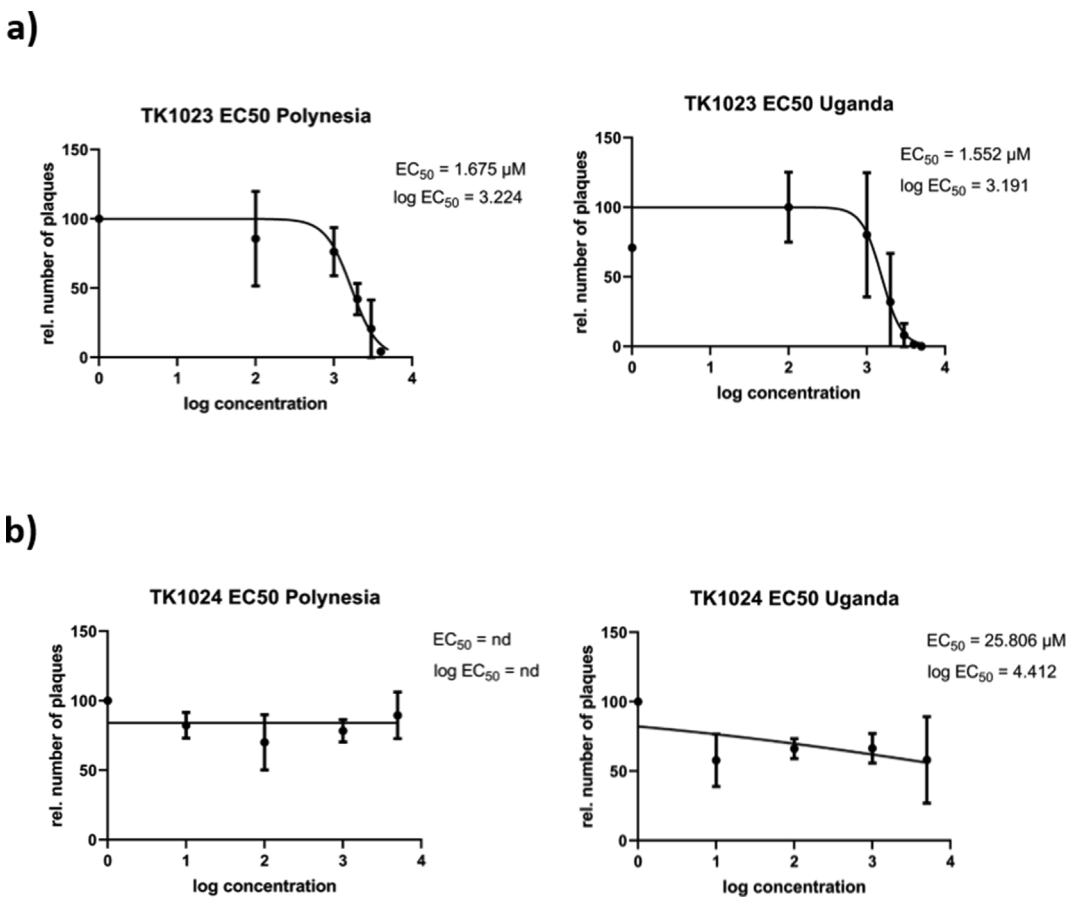

Fig. 4. IC_{50} of TK1023 on the two ZIKV isolates
A549 cells were infected with the ZIKV strains "Uganda" or "Polynesia" at an MOI of 1 and treated with 10 nM, 100 nM, 1 µM and 5 µM of TK1023 (a) or TK1024 (b) for 24 h. The number of infectious extracellular virions was quantified by plaque assay using Vero cells. DMSO-treated cells served as a negative control to calculate the respective IC_{50} values of TK1023 and TK1024.
Results are described as mean ± standard error of the mean (SEM) from 3 to 5 independent experiments.

translational inhibitor (Elgner et al., 2018), led to a slight decline in the number of ZIKV genomes until the 4 h time point, after which the infection recovers indicating the passing of the translational stage in the ZIKV life cycle. Contrary to this, no effect could be observed through the addition of TK1023 if the substance was added simultaneously to the infection or at any later time point. This suggests that the initial pre-incubation period of 2 h with TK1023 is essential to its inhibiting effect. This time period could be required for uptake and metabolic conversion of the prodrug into its active form that interferes with the entry.

However, to further dissect the mode of action of TK1023, A549 cells were infected with the ZIKV isolates "Uganda" and "Polynesia" at a lower MOI (0.1) to allow viral spread during the experiment. The amount of viral genomes was quantified by qPCR 24 hpi. The houttuynoid TK1023 was present throughout the whole experiment (TO), only during the infection (CoT), only 2 h prior to infection (Pre) or added 2 h after the infection (post). A more detailed experimental setup is schematically shown in (Gaudry et al., 2018). TK1023 is able to inhibit both ZIKV isolates on all the studied time points in this experimental setup. On the first glance this seems to argue for an inhibition of a late time point in the virus life cycle. However, due to the low initial MOI (0.1) the phenotype of this setup reflects the inhibitory effect on the viral spread. Here, in this time frame, TK1023 inhibits secondary infections by entry inhibition.

Taken together these data suggest an inhibitory effect of TK1023 on the entry process of ZIKV.

3.8. TK1023 does not inhibit acidification of endosomal-lysosomal compartments

As ZIKV infection relies on a fusion step during the entry process, it was investigated whether the effect of TK1023 on the viral entry was due to interference with the acidification of the endosomal-lysosomal compartments. For this purpose, A549 cells treated with either BFLA, a known V-ATPase inhibitor, TK1023 or DMSO as vehicle control were stained with acridine orange (Fig. 7a) 24 h after treatment. Acridine orange is a dye, which accumulates inside intact lysosomes with functional V-ATPase. Treatment with 50 nM BFLA prevented the accumulation of acridine orange in the lysosomal compartments, while the DMSO control displayed a specific dot-like distribution throughout the cells. Cells treated with 5 µM TK1023 show specific fluorescence of acridine orange in dot-like structures reflecting that acidification of the endosomal-lysosomal compartment is not abolished, Quantification of the acridine-specific staining revealed that there is no significant impact of TK1023 on endosomal acidification (Fig. 7a). .Taken together this indicates that TK1023 does not affect the acidification of endosomal-lysosomal compartments.

To investigate whether TK1023 acts on the cells or directly on the virions, the substance was incubated in a concentration of 5 µM with ZIKV virions of the "Uganda" isolate for 2 h at 37 °C. Afterwards, pre-incubated virions were diluted 1:40 before infection of A549 to reach a MOI of 1 and ensure dilution of the drug below working concentration. Pre-incubation of virions with 50 nM BFLA served as control as it is well established to act on the cells rather than on the virions (Sabino et al.,

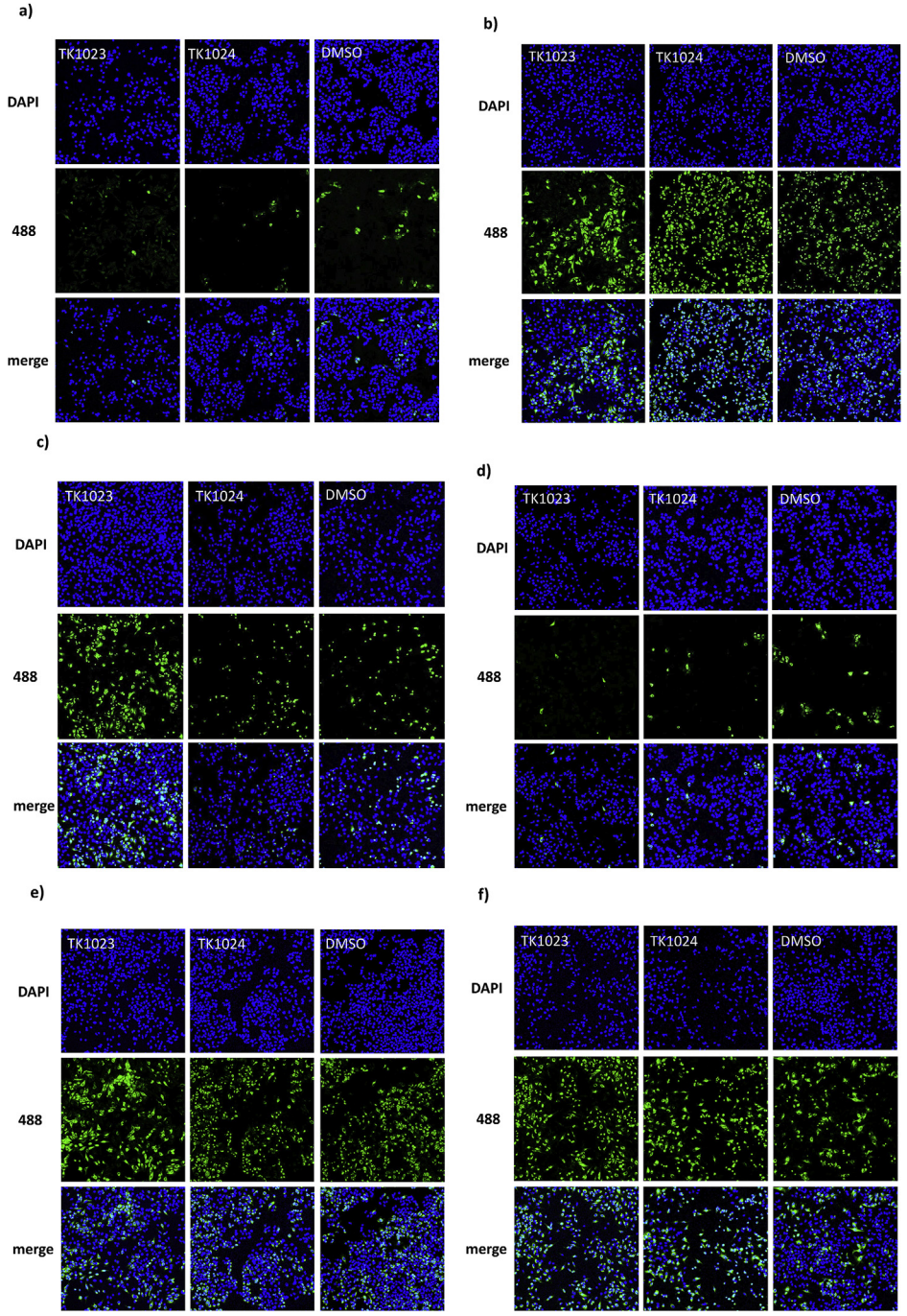

Fig. 5. TK1023 delays infection process of ZIKV
A549 cells were infected with the ZIKV strains "Polynesia" (a–c) or "Uganda "(d–f) or at an MOI of 0.1 and treated with 5 μM of TK1023, TK1024 or DMSO (0.1%) as control. The cells were fixed with 4% formaldehyde 24 h (Fig. 5a, d), 48 h (Fig. 5b, e) and 72 h (Fig. 5c, e) after infection and the number of positive cells was determined by immunofluorescence microscopy using an NS1-specific antiserum (green). Nuclei are visualized with DAPI in blue. The images were obtained with a confocal laser scanning microscope (LSM510, Zeiss).

2019). Quantification of viral genomes by qPCR 24 hpi revealed that pre-incubation of the virions with TK1023 had no inhibitory effect. This indicates TK1023 is acting on the host cell (Fig. 7b) and not on the virus.

3.9. TK1023 impairs WNV and HEV infection

To further characterize TK1023, we investigated a possible effect of TK1023 on other viruses. The impact on West Nile Virus (WNV), which is closely related to ZIKV, on Hepatitis C Virus (HCV), a relative in the *Flaviviridae* family, and on Hepatitis E Virus (HEV), a non-enveloped virus, was analyzed. As HEV exists as quasi-enveloped virus, naked virus was prepared by taurocholate treatment and subsequent density gradient centrifugation. For details see in the methods section. The obtained data were compared to experiments conducted with ZIKV Uganda.

TK1023 impairs WNV infection as evidenced by a significant decrease in infectious viral particles for WNV when compared to the DMSO control (Fig. 8a). However, no impact on the HCV infection was detected. No change in the number of viral genomes was measured for

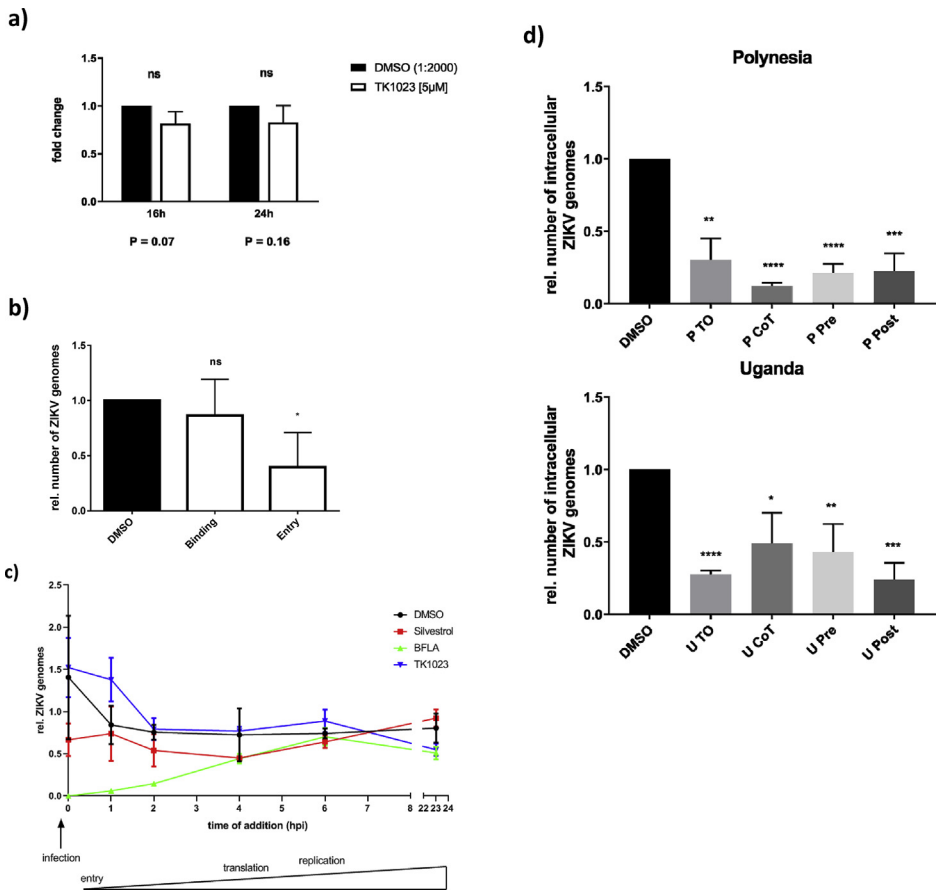

Fig. 6. The houttuynoid TK1023 acts on the entry process

(a) A549 cells stably replicating the luciferase reporter virus were treated with 5 µM TK1023. The effect on viral replication was analyzed by determination of the luciferase activity. The graph shows the relative values referred to the DMSO-treated control.

(b) Binding and entry assay. Binding: A549 cells were pre-chilled for 30 min a 4 °C before infection with the ZIKV strain "Uganda" at an MOI of 1 and subsequent treatment with 5 µM of TK1023 for 1 h at 4 °C. Intracellular ZIKV genomes were quantified by qPCR. Entry: A549 cells were infected with the ZIKV strain "Uganda" at an MOI of 1 for 4 h at 37 °C in presence of 5 µM of TK1023. Bound virions were removed by trypsin treatment for 30 s at room temperature. Intracellular ZIKV genomes were quantified relative to a house keeping gene by qPCR.

(c) A549 cells were infected with the ZIKV strain "Uganda" at an MOI of 1. The cells were treated with the substances DMSO (0.05%), silvestrol (5 nM), BFLA (50 nM) or TK1023 (5 µM) at the indicated time points post-infection. The amount of intracellular ZIKV genomes was quantified 24 hpi relative to a house-keeping gene by qPCR.

(d) A549 cells were infected with the ZIKV strains "Polynesia" or "Uganda at an MOI of 0.1 and the amount of intracellular ZIKV genomes was quantified 24 hpi. The substance TK1023 was present in a concentration of 5 µM throughout the whole experiment (TO), only during the 2 h infection (CoT), 2 h prior to infection (Pre) or added after the infection (Post). P = ZIKV Polynesia; U = ZIKV Uganda

Results are described as mean ± standard error of the mean (SEM) from 3 independent experiments. The significance of the results was analyzed by Student's t-test. ns = not significant; $p > 0.05$; *$p < 0.05$; ***$p < 0.001$; ****$p < 0.0001$.

HCV over the time frame of 72 h (Fig. 8b). However, HEV infection was affected by TK1023. The treatment of cells infected with HEV resulted in a lower number of viral genomes when compared to the control (Fig. 8c). These data indicate that TK1023 affect enveloped and non-enveloped viruses. In case of HEV it can not be excluded that secondary infections based on de novo formed quasi-enveloped particles are affected. The heterogenicity of the (non)-targeted viruses argues against a general antiviral effect of TK1023.

4. Discussion

This study aimed to investigate a potential antiviral effect of houttuynoid B (TK1024) and its tetra-acetylated derivative (TK1023) on ZIKV. Treating cells with the synthetic houttuynoids TK1023 and TK1024 2 h prior to the infection with ZIKV revealed an antiviral effect of TK1023. In a recent report, it was shown that the natural product (TK1024) results from hydrolytic deacetylation of the glycoside moiety from TK1023, which therefore might be considered as a prodrug (Kerl et al., 2016). Our analysis here revealed that the "prodrug" (TK1023) harboring the acetylated glycoside moiety has a strong antiviral activity in contrast to the putative active substance TK1024. The acetylation might lead to a higher hydrophobicity and thereby enable an easier translocation across the cellular membrane. This finally allows for a more efficient uptake of the substance that can be further metabolized by enzymatic deacetylation to the active substance.

Our data indicate that the houttuynoid TK1023 has a robust and specific antiviral effect on both ZIKV isolates. At the chosen concentration of 5 µM no impact on the cell viability was observed over the time frame of 72 h even when renewing the drug over the time course tested. This concentration was chosen to avoid any overlap with unspecific effects that could result from observed toxicity at higher concentrations. Furthermore, the CC_{50} value for TK1023 (6.3 µM) and TK1024 (42.5 µM) was higher than the concentration used in the experiments. Other studies used considerably higher concentrations to analyze the impact of houttuynoids on the HSV-1, HSV-2 and VZV life cycle in HeLa, Vero, MDCK cells and MeWo cells. In these studies, IC_{50} values in the range of 20–30 µM were observed (Lyu et al., 2005; Li et al., 2017), while similar concentrations of the substances TK1023 and TK1024 proved to exhibit a cytotoxic effect on A549 cells. Here, we observed an EC_{50} value of 1.675 µM and 1.552 µM for TK1023 for the Polynesia and Uganda strain, respectively. The EC_{50} value of TK1024 was considerably higher for the Uganda strain (25.8 µM) and could not be determined for the Polynesia strain. The low selective index for TK1023 indicates that TK1023 represents a "prototype" compound-therapeutical application might require development and characterization of derivatives with a higher selective index.

Although the substance was present throughout the experiment, the antiviral effect of TK1023 seems to disappear over time, which indicates the mode of action. The effect of TK1023 is not based on a direct effect on genome replication or virus morphogenesis during the ZIKV life cycle. This was confirmed through the observation of the application of TK1023 on already infected cells does neither affect the intracellular amount or subcellular distribution of viral proteins. Most strikingly, treatment of cells that replicate a luciferase reporter virus

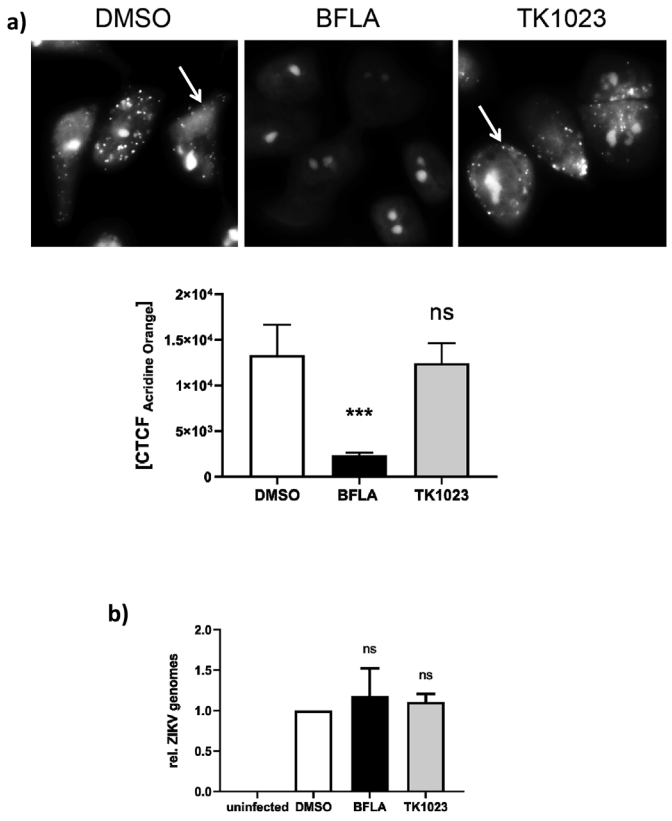

Fig. 7. TK1023 does not act on endosomal acidification or on the ZIKV virions

(a) A549 cells were treated with DMSO, 50 nM BFLA or 5 µM TK1023 for 24 h without previous starvation. Then the cells were stained with 1 µg/ml acridine orange for 15 min at 37 °C to visualize acidic compartments in the Cy3 channel. For clarity reasons the background signal level of unstained cells was subtracted. The big spots do not represent endosomal structures, typical endosomal structures are marked with a white arrow Total fluorescence per cell was calculated using ImageJ software and the following formula: corrected total cell fluorescence (CTCF) = integrated density - (area of selected cell x mean fluorescence of background readings). In total, a minimum of ten cells were measured.

(b) ZIKV Uganda was pre-incubated with DMSO, 50 nM BFLA or 5 µM TK1023 for 2 h at 37 °C. The pre-incubated virus was then diluted 40-times to infect A549 cells with an MOI of 1 and to dilute the active substance below the working concentration. Intracellular ZIKV genomes were quantified relative to a house-keeping gene by qPCR 24 hpi

Results are described as mean ± standard error of the mean (SEM) from 3 independent experiments. The significance of the results was analyzed by Student's t-test. ns = not significant.

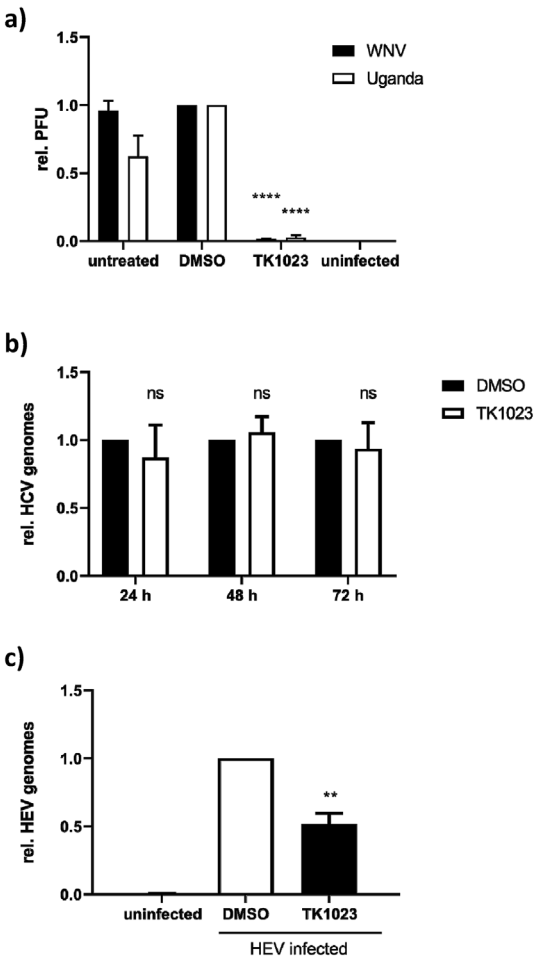

Fig. 8. TK1023 inhibits also West Nile Virus and Hepatitis E Virus but not Hepatitis C Virus

(a) Vero E6 cells were infected with the ZIKV strain "Uganda" or with WNV at an MOI of 1 after pre-treatment for 2 h with 5 µM of TK1023 or DMSO (0.05%). The number of infectious extracellular virions at 24 hpi was quantified by plaque assay using Vero cells.

(b) Huh7.5 cells were transfected with in vitro transcribed HCV Jc1 RNA and treated with 1 µM TK1023 or DMSO. The amount of intracellular HCV genomes was quantified by qPCR after 24, 48 and 72 h.

(c) A549 cells were infected with non-enveloped HEV at an MOI of 10 after pre-treatment for 2 h with 5 µM of TK1023 or DMSO (0.05%). The amount of intracellular HEV genomes was quantified by qPCR 24 hpi.

Results are described as mean ± standard error of the mean (SEM) from 3 to 4 independent experiments. The significance of the results was analyzed by Student's t-test. ns = not significant; $p > 0.05$; *$p < 0.05$; ***$p < 0.001$; ****$p < 0.0001$.

does not result in a decrease of the luciferase activity, confirming that an established infection is not affected by TK1023.

Our data conforms to the hypothesis suggesting that TK1023 interferes with the early steps of the infection process. Attachment assays revealed that the binding of ZIKV to the surface of permissive cells is not affected by the presence of TK1023. In contrast to this, we observed that the release of the internalized viral particle in the cytoplasm is impaired by TK1023. This fits to a recent observation that the flavonoid isoquercitrin exerts an antiviral effect that is mainly based on an interference of the substance during the entry process of ZIKV. As quercetin fails to exert an antiviral effect, it is concluded that the antiviral effect of isoquercitrin depends on the sugar moiety (Gaudry et al., 2018). ZIKV, as other flaviviruses, is internalized by receptor mediated endocytosis. Although the detailed steps of the escape from the endocytic compartment are not fully understood, it can be assumed that there is a fusion event of the ZIKV envelope with the endosomal membrane enabling the release of the nucleocapsid into the cytoplasm. The detection of the decreased number of viral genomes released into the cytoplasm of TK1023-treated cells is in accordance with the recently described observation that houttuynoids impair infection by blocking viral membrane fusion for HSV-1. This could reflect a more general mechanism that seems to affect a variety of enveloped viruses. Some synthesized houttuynoids demonstrated an antiviral effect on HSV-1, HSV-2 and VSV, while plant extract of *H. cordata* possesses the capability to impair the infection of a variety of enveloped viruses (Lyu et al., 2005; Chen et al., 2012; Li et al., 2017).

However, an effect of TK1023 on the acidification of endosomal-lysosomal compartments could be excluded through the use of acridine orange with BFLA as positive control. The staining by acridine orange clearly shows the presence of acidic compartments for TK1023-treated cells, while no acidic compartments were stained in BFLA-treated cells.

It is important to consider that in Fig. 7a the smaller dots exemplarily labeled by an arrow represent the acidified endosomes. To further elucidate the effect of TK1023, cells were infected with different viruses, one closely related to ZIKV (WNV), one of the same family (HCV) and one non-enveloped virus (HEV). Analysis revealed that an inhibitory effect of TK1023 was present for WNV and HEV, but not for HCV. However, cells transfected with HCV were only treated with a concentration of 1 μM, as higher concentrations of TK1023 are cytotoxic in Huh7.5 cells. This could indicate that the mode of action does not solely relate to enveloped viruses. However, as HEV is released as a quasi-enveloped virus (Himmelsbach et al., 2018) it cannot be excluded that TK1023 could act on newly produced quasi-enveloped viral particles and hinder the secondary spread of HEV. In a previous publication, no inhibitory effect of *H. cordata* extract on the non-enveloped viruses poliovirus and coxsackievirus was observed (Hayashi et al., 1995). But it should be mentioned that both viruses can be released in a non-lytic fashion with autophagic membranes (Münz, 2017).

A possible interference during the early post-entry step could explain the disappearance of the antiviral effect of TK1023 over time. Fig. 5 shows that the treatment does not completely prevent the establishment of infection as evidenced by the presence of ZIKV positive cells. A complete block might not have been achieved due to the low concentration of TK1023 that was chosen to avoid any overlap with unspecific, cytotoxic effects. The de novo synthesized viral particles aid further spread by enabling secondary infections. Indeed, at 48 hpi, a strong increase in the number of NS1-positive cells could be observed during TK1023 treatment (Fig. 5b, e). It is important to consider that the strongest production of viral NS proteins occurs within the first 24 h after infection of a cell and then diminishes over time. This explains the stronger intensity of the NS1-specific signal for the secondary-infected cells that are within this time frame. At the 72 h time point, almost all cells were positive for NS1 independent of the treatment (Fig. 5c, f). Like before, the NS1-specific signal is stronger in cells infected at later time points due to secondary infection processes compared to cells in the untreated control, where infection was not hampered and almost all cells were infected at the start point of the experiment. This is in accordance to the observation that over the infection time of 72 h the NS1-specific signal decreases. Moreover it should be considered that ZIKV can be transmitted by cell to cell spread that might not be affected by the compound.

To discern the time point that the compound stops exerting its antiviral effect, time-of-addition-assays were performed. Addition of TK1023 at the time of infection or at different time points post-infection did not lead to any observable effect on ZIKV infection if the infection was performed with a high MOI (=1). As in these assays the treatment did not occur previous to the actual infection, uptake and subsequent conversion of the compound (prodrug) in its active form (drug) by the cells could have been too slow. This could prevent the establishment of the inhibitory potential before the infection has been already established. This indicates that a treatment with TK1023 2 h before infection is necessary for the substance to be internalized and converted to its active form. This hypothesis is supported by the results of the time-of-addition experiment performed with a low MOI (=0.1). In this setup, TK1023 is able to inhibit ZIKV if it is present, before, while or after infection because there is always enough time for internalization and conversion to the active form that is able to prevent secondary infections by entry inhibition. Taken together, these results indicate that TK1023 acts as an early inhibitor of ZIKV infection by inhibiting the entry process. The substance acts on the cells and is unable to inhibit or clear an established infection.

Due to the lack of specific antivirals against ZIKV, houttuynoids represent a potentially interesting class of compounds to be used to control the spread of ZIKV.

Funding

This research was funded by a grant from the Federal Ministry of Health (BMG) to E.H. and by a grant from the LOEWE Center DRUID (Novel Drug Targets against Poverty-Related and Neglected Tropical Infectious Diseases) to D.B. and E.H. This publication was supported by the European Virus Archive goes Global (EVAg) project that has received funding from the European Union's Horizon 2020 research and innovation program under grant agreement No 653316. Based on this funding, EVAg provided the ZIKV Uganda 976 strain.

Declaration of competing interest

None.

Acknowledgments

The authors thank Gert Carra for his exceptional technical support and Frauke Hüls and Dane Junkin for carefully reading the manuscript. The authors also thank Dr. Dider Musso, Director of the Research and Diagnosis Laboratory, Institute Louis Malardé in Papeete, Tahiti, for donating the ZIKV French Polynesia strain (PF 13/251013–18).

References

Baronti, C., Piorkowski, G., Charrel, R.N., Boubis, L., Leparc-Goffart, I., de Lamballerie, X., 2014. Complete coding sequence of zika virus from a French polynesia outbreak in 2013. Genome Announc. 2 (3).

Cao-Lormeau, V.M., Blake, A., Mons, S., Lastere, S., Roche, C., Vanhomwegen, J., Dub, T., Baudouin, L., Teissier, A., Larre, P., Vial, A.L., Decam, C., Choumet, V., Halstead, S.K., Willison, H.J., Musset, L., Manuguerra, J.C., Despres, P., Fournier, E., Mallet, H.P., Musso, D., Fontanet, A., Neil, J., Ghawché, F., 2016. Guillain-Barré Syndrome outbreak associated with Zika virus infection in French Polynesia: a case-control study. Lancet (London, England) 387 (10027), 1531–1539.

Cao-Lormeau, V.-M., Roche, C., Teissier, A., Robin, E., Berry, A.-L., Mallet, H.-P., Sall, A.A., Musso, D., 2014. Zika virus, French polynesia, South pacific, 2013. Emerg. Infect. Dis. 20 (6), 1085–1086.

Chen, S.-D., Gao, H., Zhu, Q.-C., Wang, Y.-Q., Li, T., Mu, Z.-Q., Wu, H.-L., Peng, T., Yao, X.-S., 2012. Houttuynoids A-E, anti-herpes simplex virus active flavonoids with novel skeletons from Houttuynia cordata. Org. Lett. 14 (7), 1772–1775.

Coutard, B., Barral, K., Lichière, J., Selisko, B., Martin, B., Aouadi, W., Lombardia, M.O., Debart, F., Vasseur, J.-J., Guillemot, J.C., Canard, B., Decroly, E., 2017. Zika virus methyltransferase: structure and functions for drug design perspectives. J. Virol. 91 (5).

Dick, G.W.A., Kitchen, S.F., Haddow, A.J., 1952. Zika Virus (I). Isolations and serological specificity. Trans. R. Soc. Trop. Med. Hyg. 46 (5), 509–520.

Duffy, M.R., Chen, T.-H., Hancock, W.T., Powers, A.M., Kool, J.L., Lanciotti, R.S., Pretrick, M., Marfel, M., Holzbauer, S., Dubray, C., Guillaumot, L., Griggs, A., Bel, M., Lambert, A.J., Laven, J., Kosoy, O., Panella, A., Biggerstaff, B.J., Fischer, M., Hayes, E.B., 2009. Zika virus outbreak on Yap island, Federated States OF Micronesia. N. Engl. J. Med. 360 (24), 2536–2543.

Elgner, F., Ren, H., Medvedev, R., Ploen, D., Himmelsbach, K., Boller, K., Hildt, E., 2016. The intracellular cholesterol transport inhibitor U18666A inhibits the exosome-dependent release of mature hepatitis C virus. J. Virol. 90 (24), 11181–11196.

Elgner, F., Sabino, C., Basic, M., Ploen, D., Grünweller, A., Hildt, E., 2018. Inhibition of zika virus replication by silvestrol. Viruses 10 (4).

Faye, O., Freire, C.C.M., Iamarino, A., Faye, O., de Oliveira, J.V.C., Diallo, M., Zanotto, P.M.A., Sall, A.A., 2014. Molecular evolution of Zika virus during its emergence in the 20(th) century. PLoS Neglected Trop. Dis. 8 (1), e2636.

Gaudry, A., Bos, S., Viranaicken, W., Roche, M., Krejbich-Trotot, P., Gadea, G., Desprès, P., El-Kalamouni, C., 2018. The flavonoid isoquercitrin precludes initiation of zika virus infection in human cells. Int. J. Mol. Sci. 19 (4).

Glitscher, M., Himmelsbach, K., Woytinek, K., Johne, R., Reuter, A., Spiric, J., Schwaben, L., Grünweller, A., Hildt, E., 2018. Inhibition of hepatitis E virus spread by the natural compound silvestrol. Viruses 10 (6).

Hayashi, K., Kamiya, M., Hayashi, T., 1995. Virucidal effects of the steam distillate from Houttuynia cordata and its components on HSV-1, influenza virus, and HIV. Planta Med. 61 (3), 237–241.

Himmelsbach, K., Bender, D., Hildt, E., 2018. Life cycle and morphogenesis of the hepatitis E virus. Emerg. Microb. Infect. 7 (1), 196.

Himmelsbach, K., Hildt, E., 2018. Identification of various cell culture models for the study of Zika virus. World J. Virol. 7 (1), 10–20.

Jian, J., Fan, J., Yang, H., Lan, P., Li, M., Liu, P., Gao, H., Sun, P., 2018. Total synthesis of the flavonoid natural product houttuynoid A. J. Nat. Prod. 81 (2), 371–377.

Kerl, T., Berger, F., Schmalz, H.-G., 2016. Total synthesis of the antiviral natural product houttuynoid B. Chemistry 22 (9), 2935–2938.

Kuno, G., Chang, G.-J.J., 2007. Full-length sequencing and genomic characterization of Bagaza, Kedougou, and Zika viruses. Arch. Virol. 152 (4), 687–696.

Li, G.Z., Chai, O.H., Lee, M.S., Han, E.-H., Kim, H.T., Song, C.H., 2005. Inhibitory effects of Houttuynia cordata water extracts on anaphylactic reaction and mast cell activation. Biol. Pharm. Bull. 28 (10), 1864–1868.

Li, T., Liu, L., Wu, H., Chen, S., Zhu, Q., Gao, H., Yu, X., Wang, Y., Su, W., Yao, X., Peng, T., 2017. Anti-herpes simplex virus type 1 activity of Houttuynoid A, a flavonoid from Houttuynia cordata Thunb. Antivir. Res. 144, 273–280.

Lyu, S.-Y., Rhim, J.-Y., Park, W.-B., 2005. Antiherpetic activities of flavonoids against herpes simplex virus type 1 (HSV-1) and type 2 (HSV-2) in vitro. Arch Pharm. Res. (Seoul) 28 (11), 1293–1301.

MacNamara, F.N., 1954. Zika virus : a report on three cases of human infection during an epidemic of jaundice in Nigeria. Trans. R. Soc. Trop. Med. Hyg. 48 (2), 139–145.

Münz, C., 2017. The autophagic machinery in viral exocytosis. Front. Microbiol. 8, 269.

Sabino, C., Basic, M., Bender, D., Elgner, F., Himmelsbach, K., Hildt, E., 2019. Bafilomycin A1 and U18666A efficiently impair ZIKV infection. Viruses 11 (6).

Schuler-Faccini, L., Ribeiro, E.M., Feitosa, I.M.L., Horovitz, D.D.G., Cavalcanti, D.P., Pessoa, A., Doriqui, M.J.R., Neri, J.I., Neto, J.M.d.P., Wanderley, H.Y.C., Cernach, M., El-Husny, A.S., Pone, M.V.S., Serao, C.L.C., Sanseverino, M.T.V., 2016. Possible association between zika virus infection and microcephaly - Brazil, 2015. MMWR (Morb. Mortal. Wkly. Rep.) 65 (3), 59–62.

Shan, C., Xie, X., Muruato, A.E., Rossi, S.L., Roundy, C.M., Azar, S.R., Yang, Y., Tesh, R.B., Bourne, N., Barrett, A.D., Vasilakis, N., Weaver, S.C., Shi, P.-Y., 2016. An infectious cDNA clone of zika virus to study viral virulence, mosquito transmission, and antiviral inhibitors. Cell Host Microbe 19 (6), 891–900.

Sharma, A., Lal, S.K., 2017. Zika virus: transmission, detection, control, and prevention. Front. Microbiol. 8, 110.

WHO, 2016. WHO statement on the first meeting of the International Health Regulations (2005) (IHR 2005) Emergency Committee on Zika virus and observed increase in neurological disorders and neonatal malformations. https://www.who.int/en/news-room/detail/01-02-2016-who-statement-on-the-first-meeting-of-the-international-health-regulations-(2005)-(ihr-2005)-emergency-committee-on-zika-virus-and-observed-increase-in-neurological-disorders-and-neonatal-malformations, Accessed date: 27 May 2019.

Zanluca, C., de Melo, V.C.A., Mosimann, A.L.P., Santos, G.I.V.D., Santos, C.N.D.D., Luz, K., 2015. First report of autochthonous transmission of Zika virus in Brazil. Mem. Inst. Oswaldo Cruz 110 (4), 569–572.